1272–1280 *Nucleic Acids Research, 1997, Vol. 25, No. 6*

Synthesis and studies on the effect of 2-thiouridine and 4-thiouridine on sugar conformation and RNA duplex stability

Raju K. Kumar and Darrell R. Davis*

Department of Medicinal Chemistry, University of Utah, Salt Lake City, Utah 84112, USA

Received October 23, 1996; Revised and Accepted January 20, 1997

ABSTRACT

In order to understand the effect of 2-thiouridine (s^2U) substitution on RNA structure and the potential for stabilization of tRNA codon–anticodon interactions through s^2U-34 modification, a pentamer RNA sequence, Gs^2UUUC, was synthesized and characterized by NMR spectroscopy. The single strand contains the UUU anticodon sequence of $tRNA^{Lys}$ with flanking GCs to increase duplex stability. Regiochemical effects of uridine thiolation were determined by comparing the structure and stability of the 2-thiouridine containing oligonucleotide with an identical sequence containing 4-thiouridine (s^4U) and also the normal uridine nucleoside. Circular dichroism spectrum indicated an A-form helical conformation for Gs^2UUUC which was further confirmed by 2D ROESY NMR experiments. The duplex stability of the three pentamers complexed with a 2′-O-methyl-ribonucleotide complementary strand, $G_mA_mA_mA_mC_m$, was determined by UV thermal melting studies and by ^1H NMR spectroscopy. The duplex containing s^2U has a T_m of 30.7°C compared to 19.0°C for the unmodified control and 14.5°C for the s^4U containing duplex. The results from UV experiments were corroborated by imino proton NMR studies that show proton exchange rates, chemical shift differences, and NH proton linewidths indicative of the stability order $s^2U > U > s^4U$. The magnitude of the effect of s^2U in our model system is comparable to the 20°C stabilization observed by Grosjean and co-workers for 2-thiolation in a codon–anticodon model system composed of two tRNAs with complementary anticodon sequences [Houssier, C., Degee, P., Nicoghosian, K. and Grosjean, H. (1988) *J. Biomol. Struct. Dyn.*, 5, 1259–1266].

INTRODUCTION

Transfer RNAs are unique among the naturally occurring RNAs in that a very high percentage of the nucleosides are chemically modified (1,2). Despite the wide distribution of modified nucleosides, with few exceptions, the functional role of many of the modified nucleosides is unknown. Reviews published in recent years delineate the potential role of the modified nucleosides in many biological systems (3–5). Among the uridine modifications, 2-thiouridine (s^2U) and its C-5 derivatives are found predominantly in the wobble position of tRNAs (3). For s^2U, it has been shown that sulfur substantially stabilizes the 3′-endo sugar conformation at the nucleoside and dinucleotide level (6–9). It has also been shown that 2-thioribothymidine (s^2T) stabilizes tRNAs from extreme thermophiles (10–12), presumably through stabilization of the 3′-endo sugar conformation. Direct evidence for this in intact tRNA was not obtained, and the stabilizing properties of s^2U have not been confirmed for oligoribonucleotides mainly due to the synthetic difficulties involved in site-specific incorporation of s^2U and s^2T. Methods for s^2U incorporation involving base protection add additional synthetic steps to the phosphoramidite chemistry and therefore have not received wide use. Early attempts to incorporate s^2U phosphoramidite without base protection into RNA using the conventional reagents in the automated solid-phase phosphoramidite method have failed (13,14). As described previously, the difficulty can be overcome in a straightforward fashion by using *tert*-butyl hydroperoxide instead of I_2/water for the oxidation step in solid phase oligonucleotide synthesis (15–17). In the present study, we have used this method to synthesize oligonucleotides containing s^2U and characterized the resulting RNA stabilization using NMR, UV and CD spectroscopy.

As part of our project to investigate the influence of RNA modification on codon–anticodon interaction, we synthesized the RNA sequence Gs^2UUUC as the minimal model: the central pyrimidines form the anticodon trinucleotide modeled after $tRNA^{Lys}$ and the GCs at the end were inserted in order to impart reasonable stability for the duplex formed with the complementary strand $G_mA_mA_mA_mC_m$. The selection of the complementary strand $G_mA_mA_mA_mC_m$ instead of GAAAC was favored since the 2′-O-methyl containing sequence did not aggregate at the low temperature necessary to form stable duplex, whereas aggregation was a problem in the case of GAAAC. The 2′-O-methyl containing complementary strand also added stability to the RNA duplexes (18,19). The sequence GUUUC was used as a control for comparison with s^2U, and experiments with Gs^4UUUC helped to establish that only s^2U, and not s^4U, stabilizes Watson–Crick base-pairs in RNA duplexes. The observation that s^2U modification improves codon–anticodon fidelity in the wobble position of tRNAs (20) is explained by our observations of significant duplex stabilization upon substitution of U with s^2U.

*To whom correspondence should be addressed. Tel: +1 801 581 7006; Fax: +1 801 581 7087; Email: davis@adenosine.pharm.utah.edu

MATERIALS AND METHODS

UV spectroscopy

Samples for UV melting studies contained ~8×10^{-4} M of each duplex at one of two different salt concentrations, 100 mM NaCl and 1 M NaCl, in 25 mM phosphate buffer, 0.5 mM EDTA, pH 7.0. The T_m experiments were done on an HP 8452A spectrophotometer equipped with a 890090 Peltier temperature control unit; the temperature was increased in 1°C increments with a 1 min equilibration time. Measurements were repeated three times for each duplex, and the melting transitions were determined from the first derivative of the absorbance versus temperature curve. Thermodynamic parameters were determined from UV melting curves using the MeltFit program (21).

CD spectroscopy

Samples for CD spectroscopy were prepared at a concentration of ~35 μM in 25 mM phosphate buffer, pH 7.0, containing 100 mM NaCl and 0.5 mM EDTA. The CD experiments were done on a JASCO J-720 CD spectrometer, and the temperature was controlled with a Neslab RTE-110 refrigerated water bath and a flow-through CD cell. The temperature was allowed to equilibrate for 5 min at each temperature.

NMR spectroscopy

NMR experiments for the nucleoside derivatives were done using a Bruker AC200, 200 MHz NMR spectrometer. All NMR experiments on RNA oligonucleotides were carried out using a Varian Unity 500 MHz NMR spectrometer and a Nalorac ID500 indirect detection probe. The NMR samples contained ~2 mM RNA in 400 μl of 25 mM phosphate buffer, pH 7.0, containing 100 mM NaCl, 0.05 mM EDTA (for single strands) and in 220 μl of 50 mM phosphate buffer, pH 7.0, containing 200 mM NaCl, 0.1 mM EDTA (for duplexes). Shigemi (Allison Park, PA) microsample NMR tubes were used for the 220 μl duplex samples. Samples in D_2O were prepared by twice lyophilizing, then redissolving the aqueous samples in 99.96% D_2O and finally redissolving in either 400 μl (for single strands) or 220 μl (for duplexes) of 99.996% D_2O. 2D TOCSY, ROESY, PECOSY and heteronuclear COSY experiments were collected as hypercomplex data sets using TPPI-States phase cycling (22) and processed with Varian VNMR software. The ROESY experiments were collected using a time-shared spinlock field of ~3500 Hz (23,24). The F_2, acquisition, data were collected with 4096 total data points and 400 t_1 increments were zero-filled to 2048 total points in F_1. PECOSY (25) spectra were collected with WALTZ-16 ^{31}P decoupling and a decoupler field strength of ~500 Hz to minimize sample heating. The PECOSY data were collected with a spectral width of 2300 Hz, centered at the water frequency, with 4096 data points collected in F_2 domain and 400 t_1 increments zero-filled to 2048 data points in F_1. The proton-detected heteronuclear COSY (26) data were collected with 64 transients per increment, spectral widths of 1300 and 250 Hz in F_2 and F_1, respectively and 64 t_1 increments; the t_1 data was zero-filled to 1024 points.

Mass spectrometry

The FAB mass spectra were recorded on a Finnigan MAT 95 high resolution gas chromatography/mass spectrometer with Finnigan MAT ICIS II operating system. Electrospray ionization mass spectra were acquired using a PE Sciex (Norwalk, CT) API III$^+$ quadrupole mass spectrometer.

Synthesis

Thin layer chromatography was performed with Merck silica gel 60F-254 and Merck silica gel 60F (230–400 mesh) was used for flash chromatography. Chemical reagents were purchased from Aldrich except where noted and used without further purification. Spectral grade acetonitrile (Baxter) was used for HPLC.

5′-O-(4,4′-Dimethoxytrityl)-2-thiouridine (4). 2-Thiouridine (3.25 g, 12.5 mmol, 1 equiv.) was dried by evaporation from dry pyridine (2 × 15 ml), then dissolved in 30 ml of dry pyridine under Ar atmosphere. To this was added 4,4′-dimethoxytrityl chloride (5.0 g, 15 mmol, 1.2 equiv.) and the reaction mixture was stirred overnight at room temperature. Solvent was removed *in vacuo* and then coevaporated with toluene to remove residual pyridine. The residue was dissolved in 100 ml of methylene chloride and extracted with saturated sodium bicarbonate followed by sodium chloride. The solvent was dried over anhydrous sodium sulfate, solvent removed and the residue was purified by flash chromatography, using chloroform:methanol (95:5) to yield 5 g (70%) of compound **4** as a slightly yellow foam. m.p. 95–100°C; ^1H NMR (DMSO-d_6) 12.70 (s, 1H), 8.00 (d, 1H), 7.30 (m, 9H), 6.90 (d, 4H), 6.50 (d, 1H), 5.60 (d, 1H), 5.40 (d, 1H), 5.20 (d, 1H), 4.10 (m, 3H), 3.70 (s, 3H), 3.30 (m, 2H); FAB MS, found: 561.1708 (calculated for $C_{30}H_{30}N_2O_7S_1$, MH^-: 561.1695).

5′-O-(4,4′-Dimethoxytrityl)-2′-O-(tert-butyldimethylsilyl)-2-thiouridine (5). Compound **4** (2.8 g, 5.0 mmol, 1 equiv.) was dried by evaporation from dry pyridine (2 × 15 ml), then dissolved in 45 ml of dry pyridine under Ar atmosphere. To this was added imidazole (1.4 g, 20 mmol, 4 equiv.) and *tert*-butyldimethylsilyl chloride (0.9 g, 6 mmol, 1.2 equiv.). The solution was stirred for 9 h at room temperature. Solvent was evaporated and then further coevaporated with toluene to remove the residual pyridine. The residue was then dissolved in 100 ml of methylene chloride and extracted with saturated sodium bicarbonate followed by sodium chloride. The organic layer was separated and dried over anhydrous sodium sulfate. The solvent was removed *in vacuo*. The crude product which was a mixture of both 2′ and 3′ isomers was subjected to flash chromatography. The 2′ isomer was separated and solvent evaporated to yield 0.65 g (50%) of compound **5** as a white foam. M.p. 110–115°C; ^1H NMR (DMSO-d_6) 12.70 (s, 1H), 8.05 (d, 1H), 7.30 (m, 9H), 6.90 (d, 4H), 6.50 (d, 1H), 5.45 (d, 1H), 5.30 (d, 1H), 4.20 (m, 3H), 3.75 (s, 3H), 3.40 (m, 2H), 0.90 (s, 9H), 0.10 (d, 6H); FAB MS, found 675.2526 (calculated for $C_{36}H_{44}N_2O_7S_1Si_1$, MH^-: 675.256).

5′-O-(4,4′-Dimethoxytrityl)-2′-O-(tert-butyldimethylsilyl)-2-thiouridine-3′-(cyanoethyl N,N-diisopropylphosphoramidite) (6). Compound **5** (1.0 g, 1.5 mmol, 1.0 equiv.) was dissolved in 30 ml of dry THF under Ar atmosphere. To this was added DMAP (0.035 g, 0.3 mmol, 0.2 equiv.), and diisopropylethylamine (0.5 ml, 3.0 mmol, 2.0 equiv.). The solution was stirred while adding 2-cyanoethyl N,N-diisopropylphosphonamidic chloride (0.67 ml, 3.0 mmol, 2.0 equiv.). After 2 h, another 1.0 equivalent of 2-cyanoethyl N,N-diisopropylphosphonamidic chloride was added and the stirring was continued for 5 h. The reaction was quenched by adding 100 ml of ethyl acetate, the reaction mixture was extracted with saturated sodium bicarbonate followed by

sodium chloride. The organic layer was separated, dried over anhydrous sodium sulfate and the solvent was removed *in vacuo*. The residue was purified by flash chromatography on silica gel to yield 0.83 g (65%) of compound **6** as a white foam. The material exists as 1:1 ratio of stereoisomers about phosphorous and two chemical shifts are observed for some of the resonances. The secondary shifts are indicated in parentheses. m.p. 120–125°C; ^{1}H NMR (Acetone-d_6) 11.25 (s, 1H), 8.20(8.05) (d, 1H), 6.80–7.60 (m, 13H), 6.70 (s, 1H), 5.05(4.95) (d, 1H), 4.50 (m, 8H), 4.00 (m, 3H), 3.60 (m), 2.50–2.90 (m), 0.80–1.30 (m), 0.15 (d); ^{31}P NMR (Acetone-d_6) 151.12, 150.94; FAB MS, found: 877.3797 (calculated for $C_{45}H_{61}N_4O_8S_1Si_1P_1$, MH^+: 877.3795).

Oligonucleotide synthesis

The oligoribonucleotides were synthesized on an Applied Biosystems 394 oligonucleotide synthesizer on a 10 µmol scale using 0.05 M acetonitrile solutions of Perseptive Biosearch Expedite phosphoramidites; the s^2U amidite concentration was 0.1 M. Controlled Pore Glass supports were obtained from Glen Research, all other reagents were standard solutions (Applied Biosystems, Foster City, CA). Amidites were coupled for 30 min and for the synthesis of Gs^{2}UUUC, the *tert*-butyl hydroperoxide (10% solution in acetonitrile) oxidation step was 2 × 6 minutes. Synthesis of other sequences were carried out following the standard ABI procedure.

Deprotection

The CPG-bound RNA sequences were transferred from the column to a screw cap glass vial, to this was added 2.0 ml of NH_4OH:EtOH (3:1 v/v) and the solution kept at room temperature for 3 h. The supernatant was decanted, the support material washed with an additional 1.0 ml of NH_4OH:EtOH and the combined solutions heated at 55°C for 6 h, then lyophilized on a Speed-Vac concentrator. The dried material was treated with 1.5 ml of neat $Et_3N.3HF$ and the solution stirred at room temperature for 8 h. The reaction was quenched with 0.3 ml of water and the RNA precipitated by adding 15 ml of n-butanol and allowing the solution to stand at –20°C for 6 h. The precipitated RNA was recovered by centrifugation and dried *in vacuo*.

Purification and analysis

The oligonucleotides were desalted using a Waters C18 Sep-Pak cartridge following the procedure of Khare and Orban (27). The $G_mA_mA_mA_mC_m$, Gs^{2}UUUC and Gs^{4}UUUC oligos were further purified by anion-exchange HPLC as described by Vinayak and co-workers (28). The RNA oligonucleotides were analyzed by electrospray mass spectrometry and by enzymatic digestion followed by HPLC/mass spectrometry (15,29) and also sequenced by ESI tandem mass spectrometry (30).

RESULTS

Synthesis of modified nucleoside phosphoramidites and oligonucleotides

Synthesis of 2-thiouridine (Scheme 1) was achieved in high yields by the coupling of the bis silyl derivative of 2-thiouracil with 1-O-acetyl-2,3,5-tri-O-benzoyl-β-D-ribofuranose following the procedure of Vorbruggen (31); the hydroxyl protecting groups were subsequently removed with 2 M NH_3 in MeOH. The sugar protection and phosphoramidite synthesis follow standard literature procedures (32). The 5′-hydroxyl was then protected by dimethoxytritylation using DMT-Cl to give compound **4** in 70% yield. Treatment of compound **4** with TBDMS-Cl gave a mixture of 2′ and 3′-TBDMS derivatives, which on purification by flash chromatography yielded the pure 2′-isomer compound **5** in 50% yield. Reaction of compound **5** with 2-cyanoethyl-N,N-diisopropyl phosphonamidic chloride for 5 h at room temperature afforded the desired s^2U phosphoramidite compound **6** in 65% yield. The amidite **6** was then incorporated into RNA using the modified oxidation protocol as reported (15), which employs *tert*-butyl hydroperoxide instead of the conventional aqueous iodine reagent, for the oxidation step in solid phase automated oligonucleotide synthesis (33). The stepwise yield for the s^2U amidite coupling was >95% as evidenced by trityl assays and verified by HPLC. Deprotection and purification were carried out following published RNA protocols (28,34–36). Synthesis of the 4-triazolouridine phosphoramidite required to make the 4-thiouridine containing RNA using post-synthetic modification was accomplished by following the reported procedures starting from the commercially available uridine phosphoramidite (37,38). The 4-triazolouridine phosphoramidite was incorporated into RNA using the standard methods and the RNA was then treated with thiolacetic acid followed by the deprotection using 10% DBU/MeOH (37), which yielded the s^4U containing RNA oligonucleotide. The identity of the modified nucleosides was confirmed by electrospray mass spectrometry on the oligonucleotide, as well as

Scheme 1.

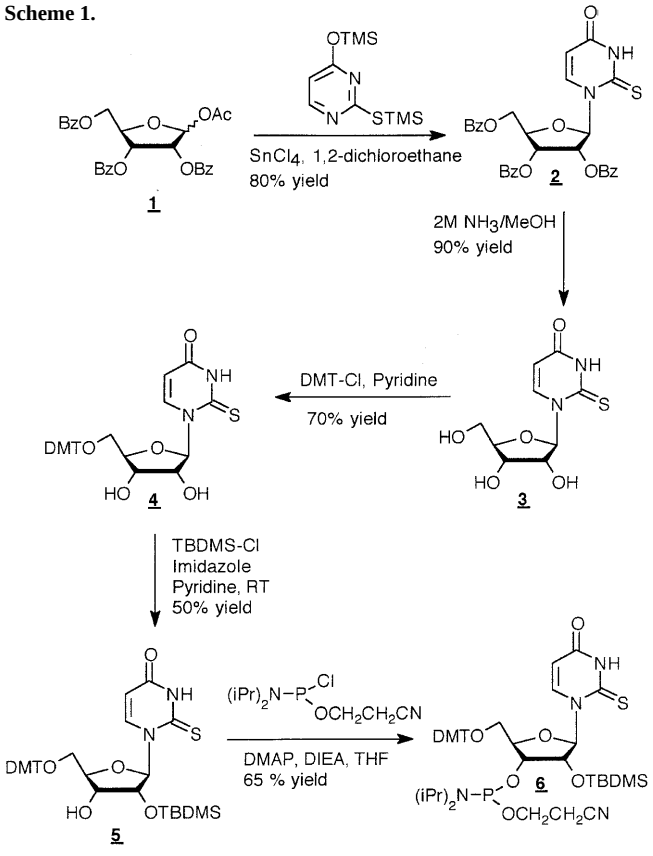

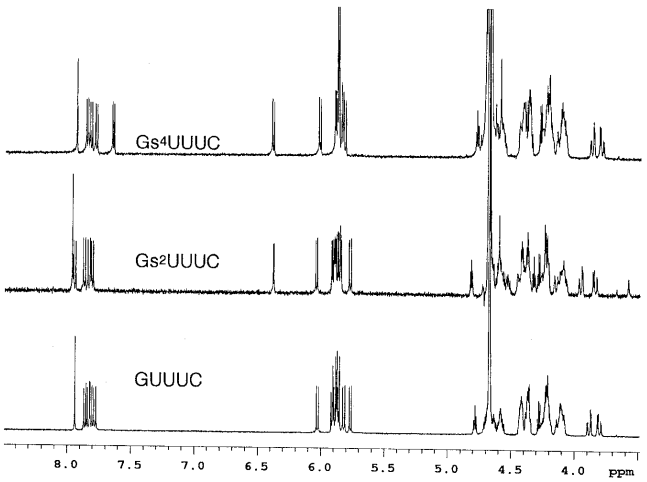

Figure 1. Proton NMR spectra at 30°C for (**A**) GUUUC, (**B**) Gs^{2}UUUC and (**C**) Gs^{4}UUUC, in 25 mM phosphate buffer, pH 7.0, containing 100 mM NaCl, 0.1 mM EDTA.

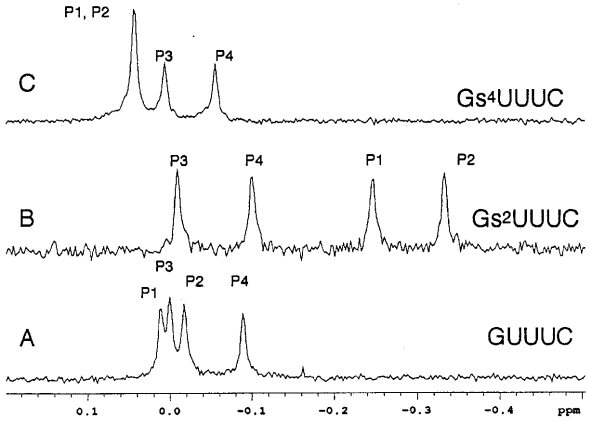

Figure 2. ^{31}P NMR spectra of (**A**) GUUUC, (**B**) Gs^{2}UUUC and (**C**) Gs^{4}UUUC, in 25 mM phosphate buffer, pH 7.0, containing 100 mM NaCl, 0.1 mM EDTA, referenced to 85% H_3PO_4

by nuclease digestion of the RNA to nucleosides followed by LC/MS (29).

NMR resonance assignments

The 1D ^{1}H NMR spectra and the ^{31}P NMR spectra of the three oligoribonucleotides GUUUC, Gs^{2}UUUC and Gs^{4}UUUC are shown in Figures 1 and 2, respectively. Resonance assignments were made using 2D NMR experiments recorded at 27°C and 30°C; the data is summarized in Table 1. The H1′ proton of the s^{2}U residue in Gs^{2}UUUC was easily identified from its characteristic downfield shift due to the sulfur substitution at C2. The H5 and H6 protons of the uridines were differentiated from the cytidine H5 and H6 protons by their different coupling constant (for uridines, $^3J_{H5–H6}$ ~8.0 Hz and for cytidine $^3J_{H5–H6}$ ~7.6 Hz). Also, the H5 resonance of cytidine was shifted downfield, and was clearly resolved from the uridine H5 resonances and the H1′ resonances (Fig. 1). For Gs^{4}UUUC, sulfur substitution at C4 resulted in a downfield shift of the H5 resonance for s^{4}U, while the H6 resonance experienced an upfield shift compared to other residues. The 5′ and 3′ terminal GCs were identified, respectively, by their characteristic downfield and upfield shifts of the H2′ and H3′ protons; it has been reported that the downfield shift of the H2′ and H3′ resonances of the 5′ terminal residue is attributed to the absence of ring current effect and the upfield shift of the corresponding resonances of the 3′ terminal nucleotide is observed due to the absence of a terminal phosphate (39). On the basis of all these starting points, assignment of the resonances for the individual residues was accomplished by a combination of TOCSY, PECOSY, ROESY and ^{1}H–^{31}P hetero-COSY experiments. Assignment of most of the resonances for GUUUC and Gs^{2}UUUC was achieved; however, extensive overlap of the central uridine resonances in Gs^{4}UUUC prevented complete assignment of this sequence.

The assignment of the ^{31}P NMR spectra (Fig. 2) for GUUUC and Gs^{2}UUUC was done by correlating the H3′ proton resonance to the ^{31}P resonances using the ^{1}H–^{31}P proton detected hetero-nuclear COSY experiment (data not shown). Assignment of the resonances for Gs^{4}UUUC was made by comparison with GUUUC and Gs^{2}UUUC since we had difficulty obtaining unambiguous assignments for the H3s as mentioned above and also because two of the phosphorus signals are overlapped as shown in Figure 2. A qualitative comparison of the ^{31}P spectra revealed that the resonances of Gs^{2}UUUC are well separated and spread over about 0.3 p.p.m. relative to the resonances from the other two sequences which appear in a very narrow region. Comparison of the spectrum for GUUUC, Gs^{4}UUUC and Gs^{2}UUUC indicated that while the resonances corresponding to P3 and P4 remain unaffected, the P1 and P2 resonances from the Gs^{2}UUUC are shifted upfield relative to the corresponding resonances from GUUUC and Gs^{4}UUUC.

Table 1. Non-exchangeable proton chemical shifts (p.p.m.) of GUUUC and Gs2UUUC at 27°C

Residue	H1′	H2′	H3′	H4′	H5′, H5″	H8	H6	H5
GUUUC								
G(1)	5.87	4.80	4.71	4.37	–	7.96	–	–
U(2)	5.92	4.38	4.65	4.44	–	–	7.82	5.77
U(3)	5.89	4.38	4.59	4.42	4.20, 4.08	–	7.79	5.83
U(4)	5.89	4.38	4.59	4.42	4.21, 4.09	–	7.84	5.87
C(5)	5.91	4.23	4.29	–	4.23, 4.12	–	7.87	6.03
Gs^{2}UUUC								
G(1)	5.82	4.79	4.57	4.34	4.12, 3.81	7.92	–	–
s^{2}U(2)	6.33	4.39	4.50	4.41	4.35, 4.13	–	7.84	6.00
U(3)	5.87	4.29	4.56	4.29	4.24, 4.06	–	7.79	5.74
U(4)	8.86	4.34	4.54	4.39	4.21, 4.09	–	7.76	5.79
C(5)	5.89	4.20	4.26	4.18	4.23, 4.08	–	7.81	5.84

Measurement of $^3J_{H1′–H2′}$ scalar couplings

It has been well established by Lee and Tinoco that the percentage 3′-endo(N-type) sugar conformation of a nucleoside in RNA is an indication of the extent of stacking for that nucleoside (40,41). Increased stacking is also predictive of a tendency to form stronger RNA duplexes when an oligo interacts with its complement (42). We measured the $^3J_{H1′–H2′}$ scalar couplings for all the residues of Gs^{2}UUUC from the 1D spectrum at 30°C (Fig. 1), where all the H1′ resonances are resolved. For GUUUC, measurements were made using the 1D spectra as well as the ^{31}P decoupled PECOSY experiment; for Gs^{4}UUUC, measurements

for the terminal GCs were possible from the PECOSY, but this data had little further utility and therefore we could not make a meaningful comparison with the other sequences. The $^3J_{H1'–H2'}$ couplings were used to calculate the percentage of the 3′-endo sugar conformation (Table 2). The limiting value of the sum of the $^3J_{H1'–H2'}$ and the $^3J_{H3'–H4'}$ couplings was set to 10 Hz based on the measurements from the ^{31}P decoupled PECOSY made at 27°C and 40°C, where both the $^3J_{H1'–H2'}$ and the $^3J_{H3'–H4'}$ cross-peaks were resolved for GUUUC and Gs^{2}UUUC. Examination of the data in Table 2 clearly indicates that the 3′-endo conformation for the s^{2}U residue is significantly stabilized compared to the comparable uridine in GUUUC. For the s^{2}U residue, the H1′ proton also remains resolved throughout the entire temperature range from 15 to 40°C, therefore the calculation of the percentage of 3′-endo pucker for this particular residue was straightforward at all the temperatures studied. Below 15°C only a singlet was observed for the H1′ proton suggesting that the sugar pucker approaches 100% 3′-endo, although we can only state definitively that the $^3J_{H1'–H2'}$ coupling is less than the 1 Hz based on a comparison of the H1′ and H8/H2 linewidths. The high percentage of the 3′-endo sugar conformation measured for the s^{2}U residue suggests that s^{2}U confers conformational rigidity to the RNA structure throughout the temperature range from 15 to 40°C.

Table 2. Percentage 3′-endo (N) conformer and equilibrium constants (N/S) at 30°C for GUUUC and Gs^{2}UUUC

	%N	%S	K_{eq}. (N/S)
GUUUC	51	49	1.0
G**U**UUC	42	58	0.7
GU**U**UC	41	59	0.7
GUU**U**C	41	59	0.7
GUUU**C**	59	41	1.4
Gs^{2}UUUC	62	38	1.6
Gs^2**U**UUC	75	25	3.0
Gs^{2}U**U**UC	77	23	3.3
Gs^{2}UU**U**C	75	25	3.0
Gs^{2}UUU**C**	61	39	1.5

The percentage of 3′-endo (N) conformers for the underlined nucleotide was calculated from %S = 100 × $J_{1',2'}/(J_{1',2'}+J_{3',4'})$, %N = 100 – %S (56).

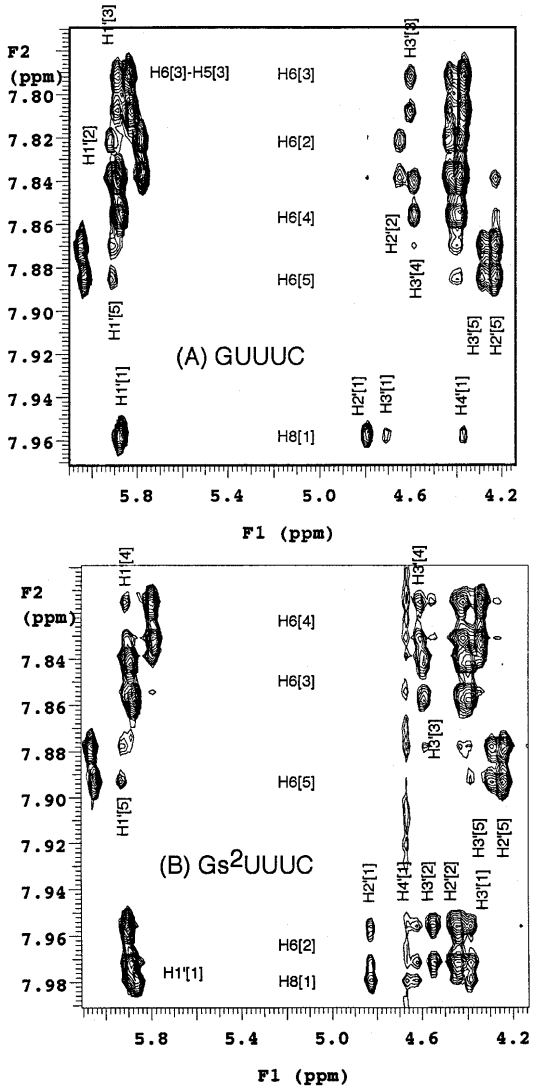

Figure 3. Base to sugar region of the 300 ms 2D ROESY spectra for (**A**) GUUUC and (**B**) Gs^{2}UUUC. Selected assignments relevant to the stacking conformation are shown, complete assignments are in Table 1. Cross-peaks from H6 protons are seen as clearly resolved doublets in F2.

2D NMR spectra of GUUUC and Gs^{2}UUUC

Although the effect of s^{2}U in stabilizing RNA structure can be seen from the sugar conformation determination, the helical structure of the RNA can be directly determined from the observation of certain NOE cross-peaks measured in the 2D ROESY NMR experiment. Comparison of the relative intensities of the cross-peaks from H8/H6 to H1′ and from H6/H8 to H2′ and H3′ reveals the preferred conformation around the glycosidic bond (43,44). Comparison of the ROESY spectra (Fig. 3) revealed that while the residues of Gs^{2}UUUC exist predominantly in the anti conformation about the glycosidic bond, a distribution of syn and anti forms is seen for the residues of GUUUC, as evidenced from the stronger cross-peak intensities from H8/H6 to H1′. In the case of Gs^{2}UUUC, the observation of a strong NOE from H6 to H2′ and the absence of an NOE to H1′ for the s^{2}U residue clearly shows that s^{2}U is strictly in the anti conformation. However, for other residues, although NOEs are observed for both H1′ and H2′ from H8/H6, the intensities of the cross-peaks to H1′ protons are weak compared to H2′ protons thereby suggesting the predominance of the *anti* conformation over the *syn* conformation.

The 2D ROESY spectra of both GUUUC and Gs^{2}UUUC shown in Figure 3 did not show many sequential NOEs for H8/H6–H1′ protons. However, intraresidue NOEs from H8/H6 to H1′ were observed. This NOE pattern could be the result of either an A-form, or a weakly stacked structure. Hence, these NOEs could not be used for any rigorous comparison. The H8/H6–H2′, H3′ region, which is more sensitive to the local RNA structure than H8/H6–H1′, was therefore used to determine structural differences. The ROESY spectra at 30°C indicated a weakly stacked structure for GUUUC and a more defined, stacked form for Gs^{2}UUUC where NOEs were observed throughout the sequence for both H2′ and H3′ to H6/H8. Observation of better stacked A-form helical structure for Gs^{2}UUUC compared to GUUUC, even at this relatively high temperature, clearly indicates the stacking stabilization effect of s^{2}U. In the case of

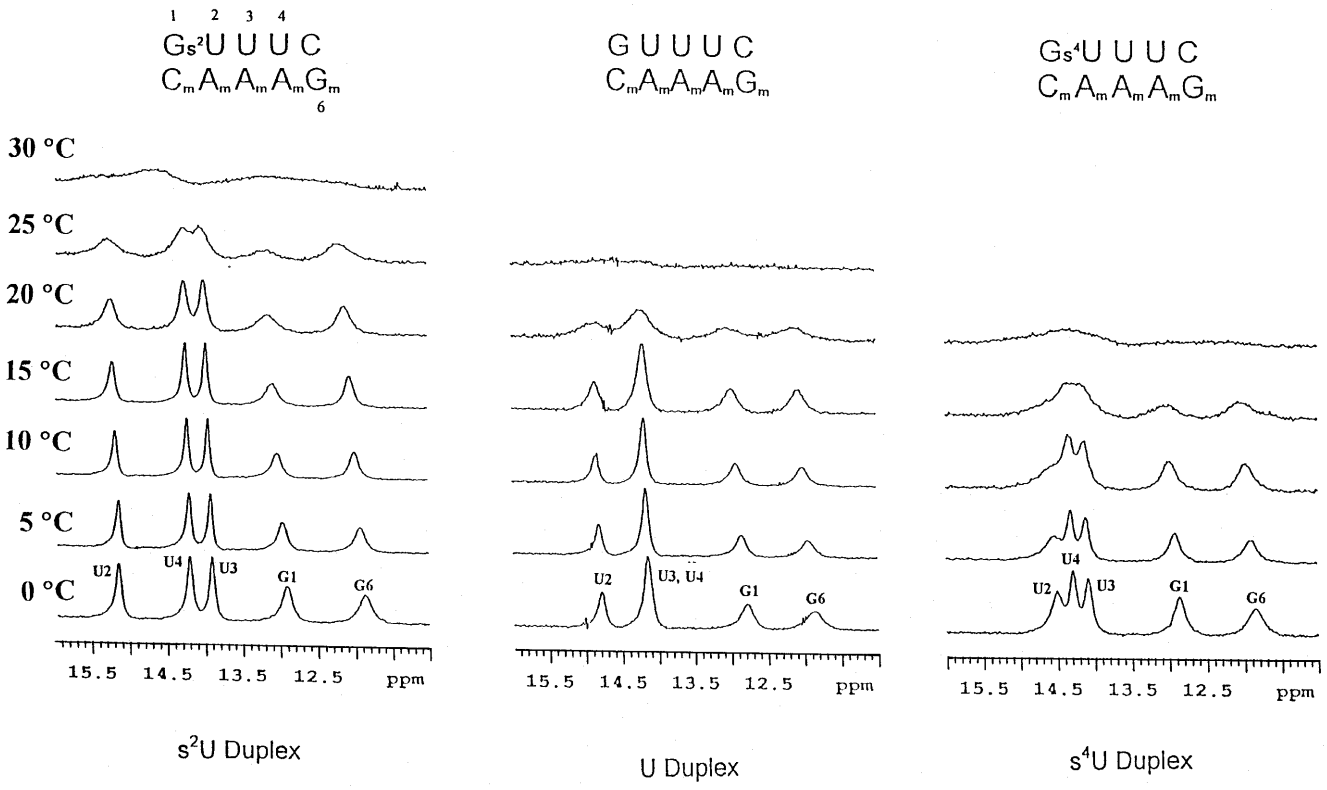

Figure 4. Downfield imino proton region of the three duplexes as a function of temperature.

Gs^{2}UUUC, cross-peaks were observed from H8/H6 to H2′, and the intensity is less than that of the corresponding cross-peaks from H8/H6 to H3′, indicating the sugars are predominantly in the 3′-endo conformation as was also indicated by the scalar coupling analysis. For Gs^{2}UUUC, this is apparent in the lower right quadrant of Figure 3 where a strong NOE was seen from the H6[s^{2}U] to H2′[G1] and a very weak NOE from H6[s^{2}U] to H3′[G1], indicating that s^{2}U forms an A-type stack with respect to G1; for GUUUC, no such NOE interaction was observed.

Duplex formation

Pentamer RNA duplexes, containing either three uridines, a single 2-thiouridine and two uridines, or a single 4-thiouridine and two uridines were prepared to assess the intrinsic effect of the uridine thiolation on base pair formation. The duplexes were generated by incremental addition of the complementary purine strand to each of the three pyrimidine strands, with observation of marker signals from both strands in the ^{1}H NMR spectrum recorded at 40°C. Although the exactly 1:1 complexes formed Watson–Crick base pairing as indicated by the imino proton resonances at low temperature, significant broadening in the aromatic region was observed (spectra not shown); this is possibly because of the tendency of the pyrimidine strands to aggregate at low temperature and hence a competition between duplex formation and self-aggregation resulted in the signal broadening. In order to overcome this aggregation problem, a slight excess of the purine strand was added to all the three duplexes which significantly improved the quality of the spectra. It has been reported earlier that in situations similar to the present study (aggregation of one of the strands in the duplex formation), addition of slight excess of the non-aggregating strand also improved the quality of the spectrum (45). The final concentration of the duplexes used for the NMR studies was 2 mM, in 50 mM phosphate buffer containing 200 mM NaCl, 0.1 mM EDTA, pH 7.0.

Temperature dependence of the imino proton NMR resonances

The downfield imino proton region of the three duplexes as a function of temperature is shown in Figure 4. While the s^{2}U and s^{4}U duplexes exhibited all five resonances corresponding to the five Watson–Crick base pairs, the unmodified duplex control showed only four resonances due to the overlap of two of the uridine imino resonances. The resonances for the s^{2}U-duplex and uridine duplex were assigned by 1D NOE difference experiments (spectra not shown). For the s^{4}U-duplex, imino resonances from the three Us were nearly overlapped, therefore the precise irradiation of the individual resonances necessary to make the NOE assignment was not possible and the assignment was made purely based on the comparison with s^{2}U and U duplexes and from the sequential disappearance of resonances due to melting effects. The imino resonances from the two terminal G–C base pairs were easily identified from their chemical shift positions compared to the A–U base pairs and also from the broad nature of the signals. The imino resonance of the s^{2}U–A base pair appeared downfield and the s^{4}U–A base pair appeared upfield compared to the corresponding resonance in the unmodified U-duplex indicating that s^{2}U forms a stronger H-bond whereas a weaker H-bond is observed for s^{4}U.

Table 3. Thermodynamic data for the pentamer duplexes

Duplex	ΔH° (kcal/mol)	ΔS° (eu)	ΔG°$_0$ (kcal/mol)	T_m (°C)
GUUUC/$G_mA_mA_mA_mC_m$	43.22	148.2	2.8	19.0
Gs^2UUUC/$G_mA_mA_mA_mC_m$	46.46	152.8	4.8	30.7
Gs^4UUUC/$G_mA_mA_mA_mC_m$	43.31	150.6	2.2	14.5

UV thermal denaturation studies of duplexes and thermodynamic parameters

The UV melting studies were carried out with two different salt concentrations, 100 mM NaCl and 1.0 M NaCl, in 25 mM phosphate buffer, 0.05 mM EDTA at pH 7.0. The duplex concentration used for melting studies was ~8×10^{-4} M. The use of such a high concentration was required for these short pentamer duplexes which exhibit very low T_ms at normal UV concentrations of 3–10 μM. Studies on such small duplexes using high concentrations for T_m measurements have been reported earlier for pentamer length RNA and DNA homo and hetero-duplexes (46). These concentrated solutions required the use of 1 mm UV cells, as well as measurements off the RNA λ_{max} of 260 nm. Hence, for the s^2U-duplex, the observation was made at 280 nm, while 270 nm was used for the U-duplex. For the s^4U duplex, the λ_{max} at 330 nm was in the measurable range and hence was used for the T_m measurement. The T_m data shown in Figure 5 and the thermodynamic parameters (Table 3) derived from the T_m data allow a quantitative measurement of duplex stability indicating that compared to the unmodified control RNA duplex (T_m = 19.0°C, ΔG°$_0$ = 2.8 kcal/mol), the duplex containing 2-thiouridine stabilizes the RNA duplex structure (T_m = 30.7°C, ΔG°$_0$ = 4.8 kcal/mol), whereas destabilization of the RNA duplex occurs upon substitution with 4-thiouridine (T_m = 14.5°C, ΔG°$_0$ = 2.2 kcal/mol).

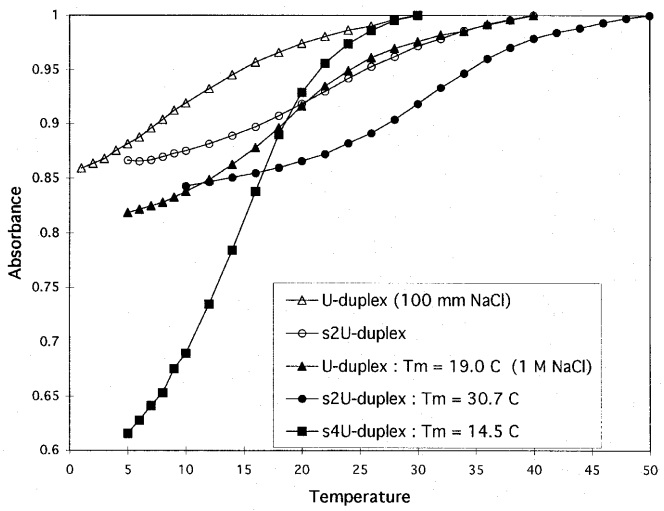

Figure 5. Normalized melting curves for the three duplexes; melting studies were carried out with two different salt concentrations, 100 mM NaCl and 1.0 M NaCl, in 25 mM phosphate buffer, 0.5 mM EDTA at pH 7.0. The duplex concentration was ~8×10^{-4} M; measurements were made at 280 nm (for s^2U duplex), 270 nm (for U duplex) and 330 nm (for s^4U duplex).

CD spectroscopy

The CD spectra of the three single strands, GUUUC, Gs^2UUUC and Gs^4UUUC were recorded at two different temperatures, 10 and 30°C , in 25 mM phosphate buffer, pH 7.0, containing 100 mM NaCl and 0.5 mM EDTA, and sample concentration of 35 μM. The CD spectra shown in Figure 6 for Gs^2UUUC exhibit a response characteristic for A-form RNA at both temperatures with a large positive band at 265 nm and a negative band near 220 nm. The negative band at 330 nm is characteristic of a thiocarbonyl group at the C2 position of uridines (47–49) which also indicates stacking in the single stranded oligonucleotide(48). The CD spectra of Gs^4UUUC and the unmodified control GUUUC have a similar profile with a positive band at 270 nm and a transition from negative to positive at 255 nm that is more typical of a B-form than A-form (46,50). For both GUUUC and Gs^4UUUC, the amplitude of the positive band at 270 nm is decreased slightly at 30°C, whereas for Gs^2UUUC the amplitude of the positive band at 265 nm did not change when the temperature was raised from 10 to 30°C. However, the amplitude of the negative band at 330 nm for Gs^2UUUC was decreased slightly on raising the temperature suggesting a partial disruption of stacking at the higher temperature.

DISCUSSION

Uridine thiolation is among the most ubiquitous and conserved modifications found in tRNAs. 4-Thiouridine is highly conserved at position 8 in eubacterial tRNA, s^2U and its five modified derivatives occupy position 34, the so-called 'wobble base' at the first position of the anticodon and s^2T is found at position 55 (1). In tRNAs having consecutive pyrimidines in the anticodon loop, the wobble base is modified to either the 2-thio or 2′-O-methyl derivatives (3), presumably to provide conformational rigidity. Previous studies to understand the role of nucleoside modification were carried out on the nucleoside and dinucleotide levels and established that s^2U preferred a 3′-endo sugar characteristic of A-form of RNA (7,9). A rigid 3′-endo sugar pucker was associated with wobble restriction of the codon–anticodon interaction, leading to the 'Modified Wobble Hypothesis' for the s^2U derivatives found at position 34 (51).

In order to find a suitable model in which to investigate the role of s^2U in codon–anticodon interactions, Grosjean and co-workers have studied the anticodon–anticodon association between *Escherichia coli* $tRNA^{Glu}$ and yeast $tRNA^{Phe}$ using the temperature jump method. They observed that the replacement of the thioketo group in the wobble position of $tRNA^{Glu}$ by a keto group lowered the melting temperature by about 20°C (20). Despite the strong role played by s^2U in stabilizing the codon–anticodon interaction, studies to investigate modification in small model systems have been limited due to the difficulties involved in the chemical synthesis of RNA containing 2-thiouridine. In the present study, a small pentamer duplex model containing s^2U is stabilized by 11.7°C compared to an unmodified control duplex, placing in context the stabilization role played by s^2U in tRNA molecules during the codon–anticodon interaction. Our NMR studies clearly indicate that s^2U favors a 3′-endo sugar pucker as shown

by the percentage of 3′-endo pucker calculated from the $^3J_{H1'-H2'}$ couplings. The effect of s^2U on the nucleoside conformation in Gs^2UUUC is propagated to the 3′ adjacent uridines which leads to stacking stabilization of the entire RNA in an A-form geometry. Such stacking stabilization of s^2U had been reported earlier for dinucleotides (9) and poly-s^2U (52), and our data show that s^2U influences the sugar conformation for the oligonucleotide Gs^2UUUC in a similar fashion to the effect described for s^2U at the nucleoside and dinucleotide level (8,9). Stabilization of A-form geometry was further confirmed by the CD spectrum of the single strand which shows that Gs^2UUUC adopts an A-form helical conformation. It has been observed earlier that RNAs containing the 5-methyl-2-thiouridine nucleoside have negative CD bands at 320–330 nm, with a shift toward the longer wavelength region for a well stacked oligoribonucleotide (48). In the present study the observation of a negative CD band at longer wavelength (330 nm) for Gs^2UUUC further confirms a stacked geometry. A partial disruption of stacking at higher temperature is shown by the decrease in amplitude of the negative band at 330 nm when the temperature is raised from 10°C to 30°C. This is in agreement with the ROESY spectrum of Gs^2UUUC recorded at 30°C (Fig. 3b), where the only sequential NOE is from H6[s^2U] to H2′[G1], while no sequential H2′(n–1)→H6(n) NOEs between other uridines are observed, indicating that there is less stacking at the higher temperature. However, Gs^2UUUC exhibits better stacking than the unmodified control GUUUC or Gs^4UUUC, even at 30°C as shown by NMR and by CD. The general A-form helical geometry is retained at 30°C for Gs^2UUUC, and is quite evident from the CD band at 265 nm which has the same amplitude at 30°C as it does at 10°C.

The observation of well separated phosphorus resonances in the ^{31}P spectrum (Fig. 2) of Gs^2UUUC relative to GUUUC and Gs^4UUUC is also an indication that Gs^2UUUC exhibits structure in solution. The shielding effect experienced by the resonances P1 and P2 (flanking the s^2U residue in Gs^2UUUC) could result from better stacking in solution compared to GUUUC and Gs^4UUUC where the backbone experiences more conformational averaging. Similarly, in the ^1H NMR spectrum of Gs^2UUUC, the H3′ proton of the s^2U residue was shifted upfield (4.50 p.p.m.) compared to the corresponding resonance from the comparable unmodified uridine (4.65 p.p.m.) of GUUUC, which again could be due to the shielding effect of the sulfur in the better stacked structure of Gs^2UUUC. 2-Thiouridine is known to have the rigid 3′-endo sugar characteristic of A-form RNA (8) and the oligoribonucleotide containing an s^2U residue exists in a well stacked conformation in which the adjacent phosphates P1 and P2 and the H3′ proton of the s^2U residue experience a net shielding effect.

The A-form geometry observed for the Gs^2UUUC single-stranded RNA is expected to result in a stabilized RNA duplex when combined with a complementary strand. It has been shown that modified nucleotides which stabilize the 3′-endo sugar lead to effective stabilization of duplexes when complexed with a complementary strand (42). NMR studies and UV melting experiments coupled with thermodynamic analysis established that s^2U containing RNA forms a very stable duplex structure whereas substitution with s^4U leads to destabilization of the RNA duplex compared to the unmodified control duplex. The relative stability of the three duplexes is also seen from the melting behavior of the imino proton resonances; the order of the observed trend of duplex stability is s^2U-duplex > U-duplex > s^4U-duplex. While these experiments provided a qualitative description of the duplex stability at the base pair level, the thermodynamic data (Table 3) extracted from the duplex melting curves furnished quantitative data on the stability of the three pentamer duplexes.

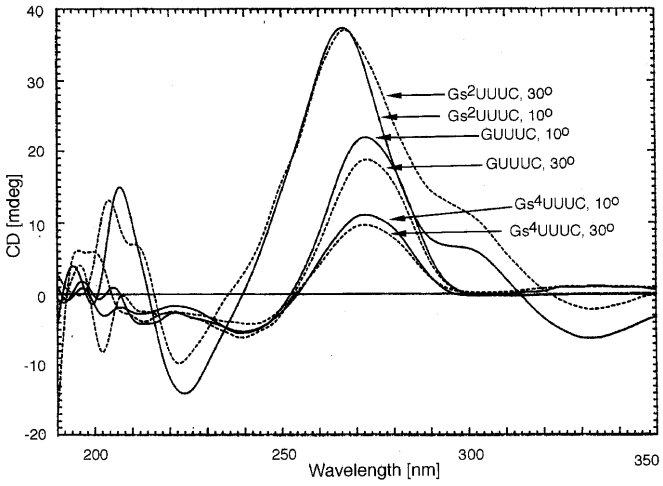

Figure 6. CD spectra for GUUUC, Gs^2UUUC and Gs^4UUUC at 10 and 30°C.

A comparison of the thermodynamic data for the three duplexes indicates that while the duplex containing the s^2U residue is stabilized by 2.0 kcal/mol, the s^4U containing duplex is destabilized by 0.6 kcal/mol relative to the unmodified control duplex. The observed trend can be explained by a combination of effects that result from sulfur modification of uridine. The reasons for the stabilization trend upon s^2U substitution include a preference for the 3′-endo sugar pucker, stacking stabilization due to the more polarizable thio group, and increased acidity of the N-3 imino proton (stronger H-bond) (53). The destabilization upon s^4U substitution is due to the lack of steric factors favoring the 3′-endo pucker, and a weaker Watson–Crick base pair due to the replacement of the hydrogen bond accepting oxygen by a weaker hydrogen bond accepting sulfur at C4. Although the s^4U imino hydrogen is more acidic (pK = 8.2) compared to s^2U (pK = 8.8) and U (pK = 9.3) and is expected to form a stronger hydrogen bond, the acidity effect is counterbalanced by the weak hydrogen bond accepting property of the sulfur at C4 involved in Watson–Crick base pairing (53). This is further supported by the fact that the imino resonance of the A–s^4U base pair appeared upfield (14.5 p.p.m.) compared to the corresponding resonance from the A–U (14.8 p.p.m.) base pair from the unmodified duplex whereas the imino resonance for the A–s^2U is shifted downfield (15.2 p.p.m.). This indicates that the s^2U residue forms a stronger hydrogen bond compared to uridine whereas a weaker hydrogen bond is observed for the s^4U residue. The observed upfield shift of the imino resonance of the A–s^4U base pair is not an intrinsic property of s^4U, but rather reflects the base-pairing geometry. The s^4U8–A14 reversed Hoogsteen base pair identified by NMR in several tRNAs has an imino resonance at 15.0 p.p.m. (54). The tRNA data support our observations with thiolated duplexes since for an s^4U–A reversed Hoogsteen base pair the pyrimidine hydrogen bond acceptor is O2. The argument we have made for the stabilizing effect of s^2U in Watson–Crick base pairs would be applicable to s^4U paired with A in a reversed-Hoogsteen geometry. The s^4U imino proton is more acidic than in U, the O2 oxygen is a good hydrogen bond acceptor, and the polarizable sulfur at C4 promotes stacking with neighboring bases.

It has been suggested that stacking of the sulfur with N1 of a neighboring nucleoside is possible in the case of s^2U containing oligomers while such stacking is not possible for the s^4U containing oligomer, and that this explains the extreme stability observed for poly-s^2U compared to poly-s^4U and poly-U (52,53). The stacking stabilization resulting from s^2U modification, the sugar conformational effect, and a shift in imino proton acidity are all effects that work synergistically to stabilize RNA structure.

Investigation of the effect of s^2U on duplex RNA structure is a necessary step for extending the published data on s^2U nucleoside and dinucleotides to more relevant systems such as the anticodon of tRNA. The duplex data presented here were designed to model the UUU–AAA interaction between the anticodon of $tRNA^{Lys}$ and an AAA codon, with as little perturbation due to flanking sequences as possible. These model duplexes show quite extraordinary increases in T_m upon substitution with s^2U. Preliminary investigations in our laboratory on an RNA tetraloop hairpin model of the codon–anticodon interaction show similar degrees of stabilization by s^2U (55). High-resolution structural studies currently in progress should provide a detailed picture of the specific structural factors that contribute to the stabilization of double stranded RNA by 2-thiouridine.

ACKNOWLEDGEMENTS

We wish to thank Jim McCloskey for helpful discussions and his group for assistance with mass spectrometry. This work was supported by NSF grant MCB-9317196 and ACS grant JFRA-405. We acknowledge the NIH for partial support of NMR and the oligonucleotide synthesis facility (RR0626, CA42014), and the NSF for mass spectrometry support (CHE-902690).

REFERENCES

1 Steinberg, S., Misch, A., Sprinzl, M. (1993) *Nucleic Acids Res.*, **21**, 3011–3015.
2 Limbach, P. A., Crain, P.F., McCloskey, J.A. (1994) *Nucleic Acids Res.*, **22**, 2183–2196.
3 Yokoyama, S., Nishimura, S. (1995) In Soll, D., RajBhandary, U.L. (ed.), *tRNA. Structure, Biosynthesis, and Function.* ASM Press, Washington, pp. 207–224.
4 Agris, P. F. (1996) In Cohn, W. M., K. (ed.), *Progress in Nucleic Acid Research and Molecular Biology.* Academic Press, pp. 74–129.
5 Bjork, G. R. (1992) In Hatfield, D. L., Lee, B.J., Pirtle, R.M. (ed.), *Transfer RNA in Protein Synthesis.* CRC Press, Ann Arbor, pp. 23–85.
6 Yokoyama, S., Watanabe, T., Murao, K., Ishikura, H., Yamaizumi, Z., Nishimura, S. and Miyazawa, T. (1985) *Proc. Natl. Acad. Sci. USA*, **82**, 4905–4909.
7 Agris, P. F., Sierzputowska-Gracz, H., Smith, W., Malkiewicz, A., Sochacka, E., Nawrot, B. (1992) *J. Am. Chem. Soc.*, **114**, 2652–2656.
8 Sierzputowska-Gracz, H., Sochaka, E., Malkiewicz, A., Kuo, K., Gehrke, C.W. and Agris, P.F. (1987) *J. Am. Chem. Soc.*, **109**, 7171–7177.
9 Smith, W. S., Sierzputowska-Gracz, H., Sochacka, E., Malkiewicz,A., Agris, P.F. (1992) *J. Am. Chem. Soc.*, **114**, 7989–7997.
10 Watanabe, K., Yokoyama, S., Hansske, F., Kasai, H., Miyazawa, T. (1979) *Biochem. Biophys. Res. Commun.*, **91**, 671–677.
11 Davanloo, P., Sprinzl, M., Watanabe, K., Albani, M., Kersten, H. (1979) *Nucleic Acids Res.*, **6**, 1571–1581.
12 Yamamoto, Y., Yokoyama, S., Miyazawa, T.,Watanabe, K., and Higuchi, S. (1983) *FEBS*, **157**, 95–99.
13 Agris, P. F., Malkiewicz, A., Kraszewski, A., Everett, K., Nawrot, B., Sochacka, E., Jankowska, J. and Guenther, R. (1995) *Biochimie*, **77**, 125–134.
14 Agris, P. C., Brown, S.C. (1995) *Methods Enzymol.*, **261**, 270–299.
15 Kumar, R. K., Davis, D.R. (1995) *J. Org. Chem.*, **60**, 7726–7727.
16 Jager, A., Engels, J. (1984) *Tetrahedron Lett.*, **25**, 1437–1440.
17 Hayakawa, Y., Uchiyama, M., Noyori, R. (1986) *Tetrahedron Lett.*, **27**, 4191–4194.
18 Inoue, H., Hayase, Y., Imura, A., Iwai, S., Miura, K. Ohtsuka, E. (1987) *Nucleic Acids Res.*, **15**, 6131–6148.
19 Kawai, G., Yamamoto, Y., Kamimura, T., Masegi, T., Sekine, M., Hata, T., Iimori, T., Watanabe, T., Miyazawa, T. and Yokoyama, S. (1992) *Biochemistry*, **31**, 1040–1046.
20 Houssier, C., Degee, P., Nicoghosian, K., Grosjean, H. (1988) *J. Biomol. Struct. Dyns.*, **5**, 1259–1266.
21 Laing, L. G., Draper, D.E. (1994) *J. Mol. Biol.*, **237**, 560–576.
22 Marion, D., Ikura, M., Tschudin, R. and Bax, A. (1989) *J. Magn. Reson.*, **85**, 393–399.
23 Kessler, H., Griesinger, C., Kerssebaum, R., Wagner, K. and Ernst, R. R. (1987) *J. Am. Chem. Soc.*, **109**, 607–609.
24 Bax, A., Davis, D.G. (1985) *J. Magn. Reson.*, **63**, 207–213.
25 Mueller, L. (1987) *J. Magn. Reson.*, **72**, 191–196.
26 Sklenar, V., Bax, A. (1987) *J. Am. Chem. Soc.*, **109**, 7525–7526.
27 Khare, D., Orban, J. (1992) *Nucleic Acids Res.*, **20**, 5131–5136.
28 Sproat, B., Colonna, F., Mulla, B., Tsou, D., Andrus, A., Hampel, A. and Vinayak, R. (1995) *Nucleosides Nucleotides*, **14**, 255–273.
29 Pomerantz, S. C., McCloskey, J.A. (1990) *Methods Enzymol.*, **193**, 796–824.
30 Ni, J., Pomerantz, S.C., Rozenski, J., Zhang, Y., McCloskey, J.A. (1996) *Anal. Biochem.*, **68**, 1989–1999.
31 Vorbruggen, H., Strehlke, P. (1973) *Chem. Ber.*, **106**, 3039–3061.
32 Damha, M. J., Ogilvie, K.K. (1993) *Methods Mol. Biol.*, **20**, 81–114.
33 Gait, M. J. (1990) *Oligonucleotide Synthesis—A Practical Approach.* Oxford University Press, London.
34 Gasparutto, D., Livache, T., Bazin, H., Duplaa., Guy, A., Khordin, A., Molko, D., Roget, A., and Teoule, R. (1992) *Nucleic Acids Res.*, **20**, 5159–5166.
35 Westman, E., Stromberg, R. (1994) *Nucleic Acids Res.*, **22**, 2430–2431.
36 Wincott, F., Direnzo, A., Shaffer, C., Grimm, S., Tracz, D., Workman, C., Sweedler, D., Gonzalez, C., Scaringe, S. and Usman, N. (1995) *Nucleic Acids Res.*, **23**, 2677–2684.
37 Shah, K., Wu, H., Rana, T.M. (1994) *Bioconjugate Chem.*, **5**, 508–512.
38 Xu, Y.-Z., Zheng, Q. and Swann, P. F. (1991) *Tetrahedron Lett.*, **32**, 2817–2820.
39 Varani, G., Tinoco, I. (1991) *Q. Rev. Biophys.*, **24**, 479–532.
40 Lee, C. H., Tinoco, I. (1977) *Biochemistry*, **16**, 5403–5414.
41 Lee, C. H., Tinoco, I. (1980) *Biophysical Chem.*, **11**, 283–294.
42 Lesnik, E. A., Guinosso, C.J., Kawasaki, A.M., Sasmor, H., Zounes, M., Cummins, L.L., Ecker,D.J., Cook, P.D., Freier, S.M. (1993) *Biochemistry*, **32**, 7832–7838.
43 Rosemeyer, H., Seela, F. (1990) *Nucleosides Nucleotides*, **9**, 417–418.
44 Rosemeyer, H., Toth, G., Golankiewicz, B., Kazimierczuk, Z., Bourgeois, W., Kretschmer, U.,Muth, H.-P. and Seela, F. (1990) *J. Org. Chem.*, **55**, 5784–5790.
45 Blommers, M. J. J., Pieles, U., Mesmaeker, A.D. (1994) *Nucleic Acids Res.*, **22**, 4187–4194.
46 Hall, K. B., McLaughlin, L.W. (1991) *Biochemistry*, **30**, 10606–10613.
47 Watanabe, K., Hayashi, N., Oyama, A., Nishikawa, K. Ueda, T., Miura, K. (1994) *Nucleic Acids Res.*, **22**, 79–87.
48 Watanabe, K., Oshima, T., Nishimura, S. (1976) *Nucleic Acids Res.*, **3**, 1703–1713.
49 Watanabe, K. (1980) *Biochemistry*, **19**, 5542–5549.
50 Sugimoto, N., Nakano, S., Katoh, M., Matsumura, A., Nakamuta, H., Ohmichi,T., Yoneyama, M., Sasaki, M. (1995) *Biochemistry*, **34**, 11211–11216.
51 Agris, P. F. (1991) *Biochimie*, **73**, 1345–1349.
52 Mazumdar, S. K., Saenger, W. (1974) *J. Mol. Biol.*, **85**, 213–229.
53 Saenger, W. (1984) *Principles of Nucleic Acid Structure*, Springer-Verlag, New York.
54 Griffey, R. H., Davis,D.R., Yamaizumi, Z., Nishimura, S., Hawkins, B.L., Poulter, C.D. (1986) *J. Biol. Chem.*, **261**, 12074–12078.
55 Kumar, R. K., Davis, D.R. (1997) *Nucleosides Nucleotides*, in press.
56 Altona, C., Sundaralingam, M. (1973) *J. Am. Chem. Soc.*, **95**, 2333–2344.